Progress in Additive Manufacturing (2025) 10:2715–2731
https://doi.org/10.1007/s40964-024-00779-7

FULL RESEARCH ARTICLE

Design and 3D printing of a customised wrist-hand orthosis

Khaled Ben Amor[1] · Sami Chatti[2] · Borhen Louhichi[3] · José Machado[4] · João Manuel R. S. Tavares[4]

Received: 17 November 2023 / Accepted: 28 August 2024 / Published online: 16 September 2024

Abstract

This study outlines a comprehensive methodology for the design and 3D printing of personalized wrist-hand orthoses. The novelty of this work consists in using a comprehensive methodology that combines 3D scanning, CAD modelling, FEM simulation, and FDM 3D printing to create a personalized wrist-hand orthosis (RO) that fits the patient's hand geometry and biomechanical requirements with an increased breathability and ventilation. It starts with a precise 3D scanning process capturing complex hand details, followed by an accurate post-processing for data refinement. Subsequently, the imported mesh model is employed in CAD software to facilitate complex modelling of the orthosis. Using a reverse engineering approach, a 3D model of the orthosis is generated, accommodating its intricate and unique shape. Fused Deposition Modeling (FDM) technology is utilized to ensure cost-effectiveness, employing PLA material, known for its biomechanical attributes. Mechanical anisotropy inherent to 3D-printed objects due to layering is assessed through tensile tests, which are conducted with specimens printed at various orientations (0°, 45°/– 45°, 90°). Following established standards, mechanical properties are derived and added into a numerical simulation employing ANSYS Workbench software. This simulation aims to optimize the orthosis's design, considering approximate wrist-level loading conditions. The resultant structure is then realized through FDM 3D printing technology. The orthosis's mechanical performance is evaluated via a 3-point bending test, consistent with prior literature standards, revealing high rigidity and load-bearing capabilities compared to existing orthotic devices. In the pursuit of ease of use, assembly and disassembly options are explored, culminating in a two-part orthosis design with a user-friendly Snap-Fit mechanism for simple use, durability, and resistance. Additionally, comfort and fitting tests validate the practicality of the design, while patients have the freedom to choose their preferred colour, enhancing the overall aesthetics and user satisfaction.

Keywords 3D printing · Reverse engineering · Orthosis manufacturing · Customized orthosis · Numerical simulation

Abbreviations

RO	Wrist-hand orthosis
FDM	Fused deposition modeling
O&P	Orthoses and prostheses
KO	Knee orthosis
AM	Additive manufacturing
AFO	Ankle–foot orthosis
PA	Polyamides
PE	Polyethylene
PLA	Polylactic acid
ABS	Acrylonitrile butadiene styrene
CFRP	Carbon fibre-reinforced polymer
HIPS	High-impact polystyrene
TPE	Thermoplastic elastomer
PP	Polypropylene
FEM	Finite element method
FEA	Finite element analysis

✉ Borhen Louhichi
blouhichi@imamu.edu.sa

[1] LGM-ENISo, University of Sousse, 4000 Sousse, Tunisia

[2] LGM-ENIM, University of Monastir, 5000 Monastir, Tunisia

[3] Department of Mechanical Engineering, College of Engineering, Imam Mohammad Ibn Saud Islamic University (IMSIU), 11432 Riyadh, Saudi Arabia

[4] Departmento de Engenharia Mecânica, Faculdade de Engenharia, Universidade do Porto, Rua Dr. Roberto Frias, 4200-465 Porto, Portugal

1 Introduction

An orthosis is a manufactured tool that provides external support to the spine, extremities and other body parts, reducing unwanted movement by the individual. Orthoses assist in the recovery of injured extremities and enhance their functional capabilities [1]. Prostheses are medical tools used to replace missing body parts in the upper or lower limbs. Both devices are engineered to sustain specific body parts [2]. They possess similar design features, such as being lightweight, exhibiting high compression and tension strength, having high stiffness to counteract shear stress, demonstrating high resistance during impact, and being manufactured at low cost [3]. Orthoses and prostheses (O&P) are traditionally manufactured using various methods such as hand-carving, moulding, and casting. Hand-carving involves using hand tools to shape the orthosis or prosthesis from a solid block of material. Moulding consists of creating a mould of the limb or body part and then using that mould to create the orthosis or prosthesis. Casting involves creating a mould directly from the limb or body part and then using that mould to create the orthosis or prosthesis. The traditional method for orthosis manufacturing was based on creating a gypsum shell to cover the limb. However, this method possesses several disadvantages; apart from the lack of access to the limb during the recovery period, it can affect the skin with infections, exhaustion, itching, allergic reactions, and other complications that may harm the skin. Moreover, it lacks the user's comfort and has a high weight [4].

The Industrial Revolution significantly impacted the manufacturing of orthoses and prostheses. With the advent of mass production techniques and the availability of new materials such as plastics and composites, the manufacturing of orthoses and prostheses became more efficient and cost-effective. The healthcare industry is undergoing a significant transformation, and expanding patient care through personalized products can significantly improve the quality of life for patients. Custom orthoses or prostheses enable greater comfort and reduced rates of adverse events by creating a more customized fit for each patient [5, 6]. The level of customisation plays a significant role in the success rate of the patient treatment [7]. In the realm of personalized product development, particularly in the manufacturing of orthoses and prostheses, rapid prototyping stands out as the preeminent technological approach. In this context, 3D printing has emerged as the most widely recognized method for immediate production. The medical industry has taken additive manufacturing (AM) as the leading manufacturing technology due to its ability to provide fast execution. The constantly changing nature of the human body requires constant adjustment and adaptation of the prosthesis and the orthosis production [8]. It provides high freedom of design, manufacturing complex parts with a low material usage and cost efficiency, and increased functional performance with the least weight where we can manipulate it with the printing parameters [9]. The AM, also known as 3D printing, is a manufacturing technology based on depositing the material layer by layer to form a 3D object following a digital model. This technology has been proven to have a high potential for custom manufacturing orthoses and prostheses [10]. The traditional O&P manufacturing techniques require several visits for the patient's measurement, fitting and comfort, which can take around two weeks on average to be fabricated. The AM can solve such a problem and reduce the number of clinic visits [11].

Moreover, it can make the manufacturing process more accessible, provide more design flexibility, and reduce the cost, time, and materials waste for the O&P manufacturing [12]. One additional advantage of AM technology is the ability to use finite element analysis to achieve an optimal topology while maintaining the same level of performance. This topology optimisation approach is not feasible with traditional manufacturing methods, making AM a highly desirable choice for producing complex structures. With AM, the ability to create intricate geometries and designs, coupled with the benefits of topology optimisation, allows for developing components with superior mechanical properties, reduced weight, and improved efficiency [13].

Two of the AM's different technologies were used in the O&P manufacturing. Selective laser sintering (SLS) was used in other applications such as the foot orthosis [14], ankle–foot orthosis (AFO) [15], prosthetic feet [16] and more. However, this process was costly due to the high expenses of materials and equipment [12], and when it comes to the high cyclic loadings, the SLS technology would not be selected due to the materials bending and strength resistance limitations. The fused deposition modelling (FDM) technology has proven suitable for the O&P manufacturing [17]. The fabrication process is based on giving the 3D printer an STL file which contains a certain G-code. A thermoplastic filament starts to be heated and extruded through a nozzle on a platform following the G-code, layer by layer until the final 3D object is finished. Several materials are used in the FDM technology.

The AM, especially FDM, provides many advantages compared to conventional technologies. The most important feature is its customisation manufacturing [18], the most desired quality in medical applications such as the O&P manufacturing [19]. The most crucial factor for user satisfaction is a customized product with individual characteristics that best fit his body [20]. The AM also has many advantages that were mentionned previously compared to the conventional manufacturing [21]. The high accuracy of FDM 3D printing is due to the precise extrusion of preheated plastic filaments by the nozzle at a constant speed. Depending on the type of FDM printer, the printing speed can also be relatively fast. However, research is still being conducted to improve the performance of FDM 3D printing technology [22].

However, The FDM technology possesses a significant disadvantage related to the mechanical properties of the object to be manufactured [23]. These properties are often uncertain, hard to predict, and present anisotropic behaviour. Moreover, the printing process parameters have a high influence on the mechanical properties, too. These parameters have been studied to be optimized depending on the requirements of [24, 25].

Several materials are used for orthosis manufacturing. Usually, they are merged to get the desired characteristics. Metal is used for long-lasting components, although it is weighty and not appealing. Thermoplastics are more aesthetically pleasing and have a lower weight. However, they exhibit less strength compared to metal. Thermoplastic materials are more effective for short-term uses. Low-temperature polymers may be formed directly on the body, unlike high-temperature plastics, although they are also less strong [5]. Thus, semicrystalline thermoplastic materials such as polypropylene (PP), Polyamides (PA), and polyethylene (PE) are mainly used for the manufacturing of conventional orthoses due to their suited material properties. These materials are known for their flexibility, toughness, chemical resistance, and low density [26]. H. Beckennan et al. [27] used the PP material for an AFO manufacture, this material allowed a minimal dorsiflexion caused by the material transformation and the good balance between the strength and flexibility of the material, which is essential for proper fitting and comfort of the AFO. Also, it has been mentioned by [28] that the PA 12 material in terms of flexibility and chemical resistance is better than ABS, PLA and High Impact Polystyrene (HIPS) materials. However, it has the highest manufacturing cost and comes second in terms of stress resistance after the PLA material. Each polymer material has both limitations and benefits compared to other materials. It is also possible to use composite materials in the manufacturing of orthosis with the FDM technology. J. Rybarczyk et al. [29] used both ABS and ABS with carbon fiber to print a leg orthosis. The tests confirmed an improvement in resistance by adding the carbon fibre to the material.

Concerning the materials, it has been proven that the PLA material is the best for orthosis printing. However, it can soften and weaken if used at a temperature above 60 °C [30]. The PLA is the most common 3D printing material. It is a biocompatible and non-toxic material with high stress resistance and low cost compared to other FDM printing materials. Its mechanical properties are wildly investigated, and it was proven to have anisotropic mechanical characteristics for its 3D printing Field [31, 32], making it the best material to use in our case. PLA is known for being odourless and quickly heating up, and it is less prone to deformation than acrylonitrile butadiene styrene (ABS). As a result, PLA does not require a very hot platform during the 3D printing process, which can simplify the printing setup [22].

Looking at the state of the art of this research field, we can find that R. Chen et al. [12] conducted a study comparing two AM fabricated ankle–foot orthoses (AFOs) using PC-ABS material and the Polyetherimide (PEI) also known as ULTEM material with a conventional polypropylene (PP) AFO. Their experimental results showed that the FDM AFOs had lower strain during the subject's gait. The team developed a finite element model (FEM) with both static and dynamic loading conditions to predict the strain, stress, deformation, and stiffness of the AFOs. The FDM technology was found capable of fabricating AFOs with sufficient strength and stiffness, although the durability of the FDM AFOs still needs to be tested.

Manufacturing time using FDM 3D printing of personalized orthoses and prostheses takes approximately one day. However, the research team expects this time to be reduced by incorporating optimal topology geometry and sparse structure, potentially increasing the printing process's efficiency and speed. Chen and his colleagues concluded that FDM can be a more feasible option for personalized orthoses and prostheses. M. Ali et al. [22] analyzed a finite element of a 3D-printed AFO using different FDM materials. It was concluded that the carbon fibre-reinforced polymer (CFRP) had the best mechanical performance, precisely the PLA polymer. An experimental study was made by F. Górski [28], which was based on the best material to print a wrist-hand orthosis (RO). Acrylonitrile–butadiene–styrene (ABS), polylactic acid (PLA), high-impact polystyrene (HIPS), and polyamide 12 nylon (PA12) were investigated with economical, accurate and strong printing settings. The economical settings use a 15% infill density and 0.3 mm layer thickness which is optimized for cost-efficiency and faster printing times. The accurate settings are a 15% infill density and 0.15 mm layer thickness that prioritizes high precision and detail. And the strong settings used a 90% infill density and 0.3 mm layer thickness to enhance the strength and durability of the printed object. The wall thickness they used was 4 mm, and they applied an offset between the orthosis and the patient hand geometry of 3 mm. It was found that the PLA material was the strongest. The PLA horizontal accurate strategy performed the best force break with a 1412 N value. The orthosis final modelling results are presented in Fig. 1.

Savov et al. [4] developed a rapid, automated method for personalized orthosis design. This research resulted in the creating of a computerized tool importing the scanned organ and exporting a premade model for orthosis creation. An example of the premade orthosis model is given in Fig. 2. Their method is based on two steps, the first step is to create a CAD model from the scanned organ. And by an automated macro, which creates surfaces offsetted with the the scan file to be swept and then extruded to have the premade orthosis model. The results to this model is shown in Fig. 2a. The second step is for the topology optimization by cutting the material from the premade model following a specific

Fig. 1 RO modelling results. **a** ORTHOSIS on the forearm phantom, **b** vertically manufactured orthosis using the PLA material with different strategies [(left to right): economical, accurate, strong] [28]

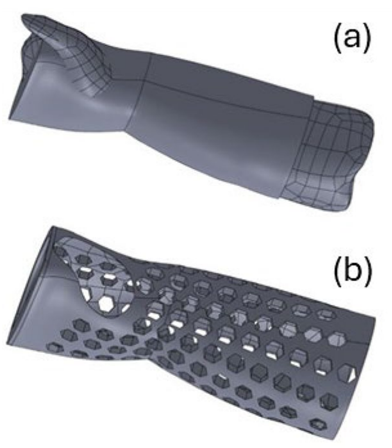

Fig. 2 Premade orthosis models creation example (**a** Non-optimized model; **b** Optimized model) [4]

mapping strategy resulting to the optimized premade model of the orthosis that is shown in the Fig. 2b. Research by A. Dal Maso and F. Cosmi [32] was based on a 21-year-old woman who had problems when walking wearing a plaster ankle–foot orthosis (AFO). They used the FDM technology to create a fully customized AFO. They used the FEM on the optimized geometry to ensure that the orthosis is resistant enough and that it sustains the foot during the load of the walk phases. Some researchers designed a flexible neck orthosis using the FDM technology with the thermoplastic elastomer (TPE) material. They also made a FEM to validate the resistance of their orthosis. The maximum enlargement was the optimum in pattern design for different loading conditions, increasing the breathability of the orthosis in use [33].

Leite et al. [34] presented a technique for producing medical parts using additive manufacturing and 3D scanning. Specifically, they aimed to develop a knee orthosis (KO) by following a process that included scanning the knee, designing the orthosis, manufacturing the device, and then conducting testing. Ultimately, they produced five prototypes, with the final one successfully meeting the initial design requirements. Notably, the final KO was more comfortable, more accessible to replace, lighter, had reduced pressure areas, and was thinner than previous versions.

William K. Durfee and Paul A. Iaizzo [35] emphasized the importance of knowing and documenting the fabrication parameters when 3D printing a medical device. Parameters such as slicing thickness, infill density, and build path can impact the device's stiffness, hardness, and yield strength. Additionally, the device's mechanical properties are influenced by its build orientation and the size and placement of support structures. Even the position of the part in the build volume can affect its mechanical properties. It is important to note that the machine software usually makes support decisions automatically and can vary between vendors. Finally, temperature and humidity in the built environment should be controlled to ensure consistent prints—the work produced by Rita Ambu et al. [36] presents a study on the design of a customized neck orthosis using fused deposition modelling (FDM) with a new sustainable biocomposite. The study aimed to develop a lightweight, ventilated, hygienic, and comfortable orthosis for neck injuries. The authors used the anatomic data of a volunteer subject to model the orthosis using CAD software. Two geometrical patterns were introduced to improve breathability and lighten the orthosis. Finite Element Analysis (FEA) was conducted to assess the structural performance of the two patterns. The study found that the elliptical pattern outperformed the honeycomb pattern regarding displacement and maximum Von Mises stress for both models under the same loading conditions. The oval holes pattern performed better than the honeycomb pattern in terms of structural performance and improved the orthosis's breathability.

With the combination of the AM technology and the FEM, the O&P manufacturing has been developing day by day. Some work used this combination to determine the cross-sectional strut dimensions of an AFO following temperature and frequency loads [15]. In another study, it was used to evaluate the performance of an AFO with additional space for the air to circulate to solve the high heat and sweating [13]. Most of the FEM studies on O&P manufacturing using the AM technology were to evaluate the strength, deformations, spot the stress areas, the best patterns, etc.

However, only some researchers used it to have the optimal topology.

RO is the most used orthosis product because the most common injuries are at the Wrist-hand level, with 25% for the paediatric population and 18% for the elderly age group [37]. In our work, we will focus on the static RO, which is based on eliminating the wrist movement at a given position.

Getting a specific shape is a time-consuming computer-aided design (CAD) modelling process [37], and the FDM process products' accuracy and strength are challenging to satisfy for the variety of parameters that impact the mechanical properties [38]. There are several designs available in the literature. However, the model needed optimization for the best topology and material distribution. The optimization process in the work done by K. Savov et al. [4] and F. Górski et al. [26] involved material removal either randomly or following a specific pattern of holes mapping. This optimization process will result in more material removal and can lead to a lighter orthosis, however, this material removal can weaken the orthosis on the stressed areas in which we need higher resistance. This point led us to this paperwork idea in which we will develop an optimized orthosis with a specific optimization depending on a certain load. The objective is then to design a customized RO with an optimized topology using finite element modelling to have an optimum material distribution that will be the distinct point compared to the literature. Our orthosis must resist the load needed with the least weight, and have the necessary fit and surface quality, which must satisfy the patient and reduce the cost and time. And then we will compare our orthosis resistance with other orthoses and show that it has the same range of resistance, is lighter and guarantees the requirements. For this objective, a study on the mechanical behaviour of the material must be carried out, and a CAD modelling strategy has to be followed, which reduces the modelling time.

2 Materials and methods

2.1 Work plan

The following scientific work plan was employed to accomplish our objective within an optimal timeframe. The list of tasks to summarize the work plan is presented in Fig. 3:

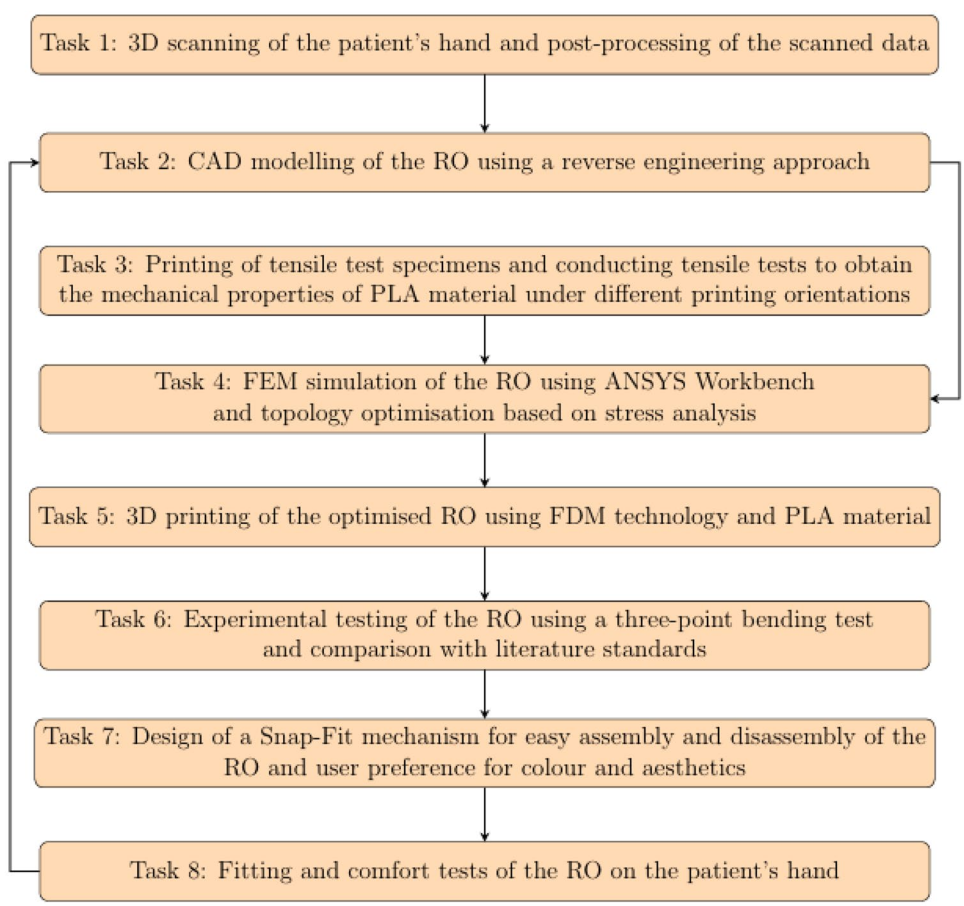

Fig. 3 Work plan flowchart

Fig. 4 Patient position during scanning process

Fig. 5 Patient hand scanning output

Fig. 6 Post-processed patient scanned hand

2.2 Scanning process

Two scanners were utilized in the scanning process: the Sense scanner and the Artec 3D scanner. It was determined that the Sense scanner yielded superior results. The scanning setup involved positioning the elbow on the edge of a chair, as depicted in Fig. 4. The outcome of the scanning process is presented in Fig. 5. The 3D Systems Sense Scanner software was used to extract the OBJ file, which was then used to fill empty areas and smooth the surface. For post-processing, the AutoDesk Meshmixer software was employed. The OBJ file was imported, cleaned, and ground as necessary, resulting in the final scanned hand, as illustrated in Fig. 6.

Fig. 7 Imported mesh file of the scanned hand in SOLIDWORKS software

2.3 CAD modeling process

The mesh, which was obtained from the hand scanning and post-processing steps and exported as a ".mesh" file, was imported into SOLIDWORKS 2020 CAD software for further analysis, as shown in Fig. 7. A slicing command was applied to the region with an offset of 10 mm for each slicing plane, resulting in multiple intersection splines between the mesh part and the slicing planes. A balance of 1 mm was applied to each spline to allow for the inclusion of a soft cloth for added comfort during use. A boundary boss feature was applied to the splines to create a solid part. An outward shell function was applied to the external surface, providing the ability to adjust the thickness of the orthosis, which was set to 2 mm in this case. These steps resulted in the orthosis CAD model shown in Fig. 8.

2.4 Filament mechanical properties investigations

When it comes to the material choice for this investigation, it is possible to use different materials from PLA, ABS, PETG and other polymers. Also, we can work on dual materials such as composite materials which can reinforce our orthosis and enhance its properties. However, we have chosen the PLA material in our investigation due to its recommendation in most of the literature and due to its availability in the market, with a low price, ease of use, and its sustainability.

In this study, we used PLA filament from “Filament PM”, a supplier based in Portugal. The PLA filament is white with a diameter of 1.75 mm. It requires a nozzle temperature range of 190–210 °C and a bed temperature of 60 °C for optimal printing conditions.

This study investigates the mechanical behaviour of our 3D-printed PLA material by printing tensile test specimens. The specimens were used to extract the material's mechanical properties, which were then incorporated into a numerical model. This information is crucial for understanding the capabilities of 3D printed PLA material and is used to optimize the design and manufacturing process for the orthosis. For this purpose, we used the software SolidWorks for the CAD modeling. By saving the file into an STL format, we imported it into ideaMaker slicing software to manipulate the printing parameters. We used a white PLA material provided by Filament PM for the printing and using the ORIGINAL PRUSA i3 MK3 printer.

To evaluate the effect of printing orientation on the tensile properties of PLA material, four specimens were fabricated for each of the following orientations: 00°, 45°/– 45°, and 90°. The printing parameters, including layer height (0.15 mm), printing speed (60 mm/s), infill density (100%), printing temperature (210 °C), and bed temperature (60 °C), were held constant throughout the experimentation.

The ASTM D638-02a [39] (Type I specimen, with 4 mm thickness) standard was utilized to conduct tensile testing with the dimensions given in the Fig. 9.

The tensile testing was performed using the MTS 810 machine. The testing speed was by the ASTM standard at 5 mm/min. The results of this study are presented in Fig. 10, which illustrates the 3D-printed tensile specimens with different orientations.

A total of four specimens were tested for each printing orientation, and the results were found to be consistent. The mean values of the curves were calculated and

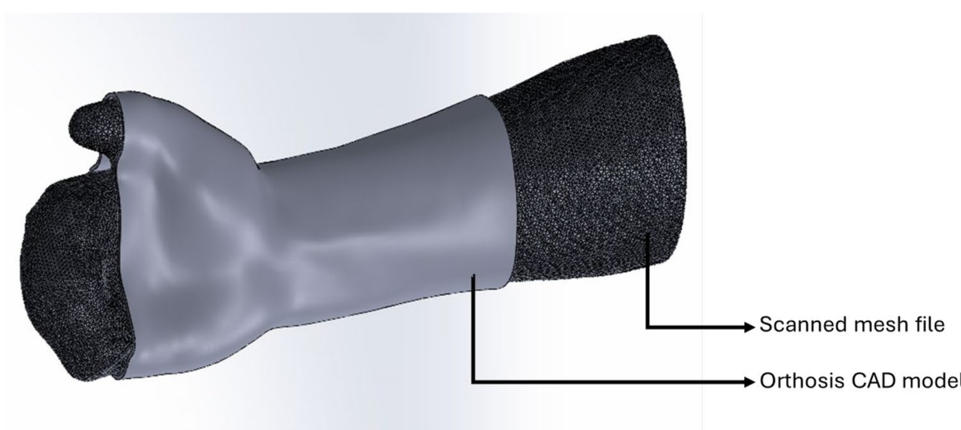

Fig. 8 Orthosis first CAD model

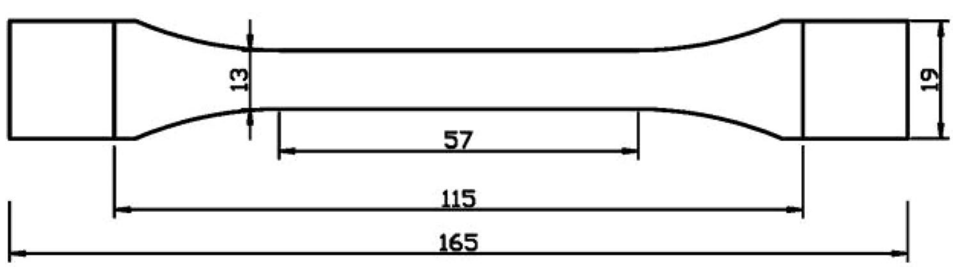

Fig. 9 ASTM D638-02a standard dimensions in mm [39]

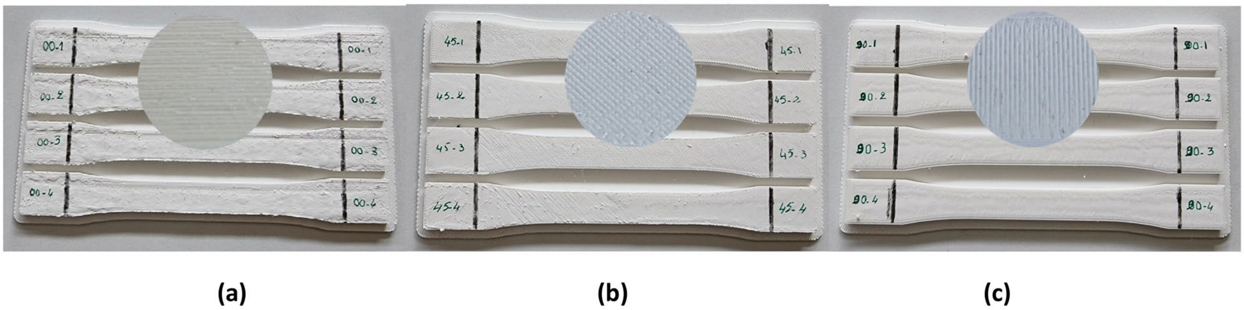

Fig. 10 3D printed tensile test specimens for each printing orientation. The circular images show a zoomed-in view of the printing orientation. (**a** 00°, **b** 45°/– 45°, and **c** 90°)

compared to determine the impact of printing orientation on the mechanical properties of the printed material.

2.5 Topology optimization

This study aims to conduct a numerical simulation of a wrist-hand orthosis model by applying realistic loads and visualising the areas of high-stress concentration. The simulation was performed using ANSYS Workbench 2021 R2, which provides a fast computation time and easy mesh manipulation depending on the needs. The process involved importing a CAD orthosis model and incorporating the mechanical properties of PLA material as determined by tensile testing. Equations 1 and 2 [43] were applied to the stress and strain data obtained from the testing to ensure the results were rational.

The simulation used boundary conditions and loads that mimicked real-world situations. Utilizing the muscle groups and parameters for muscle modelling investigated by K. R. Holzbaur et al. [40], the analysis allowed for the calculation of the maximal force generated during various wrist movements. Wrist flexion emerges as the most robust movement, demonstrating a force of 304.9 N. Subsequently, the extension movement yields a maximal force of 100.5 N, trailed by radial deviation at 74 N, and ulnar deviation registering a maximum force of 128.9 N. Considering the intricate nature of force modelling in diverse applications, we chose to simplify the simulation by treating it as a flexion force at the wrist, we applied these forces at the wrist level. Additionally, we fixed both ends of the orthosis pointed with blue and conducted the optimisation process under these conditions as Fig. 11 shows.

The mesh used for the simulation was a triangular quadratic interpolation with a mesh size of 1 mm, enabling us to obtain more reliable and realistic results for the topology optimisation process.

The results of the simulation are presented in Fig. 12.

$$\text{Rational or real stress} : \sigma = R \times (1 + e) \tag{1}$$

$$\text{Rational or real strain} : \varepsilon = \ln (1 + e). \tag{2}$$

With σ: real stress, ε: real strain, R: conventional stress and e: conventional strain.

The results presented in Fig. 12 show the distribution of the stress over our model which was subjected to the loads mentioned. Most of the stress is located at the wrist area and a portion of the stress is located at the sides.

The ANSYS Workbench software was selected for the numerical investigation because it enables the selective manipulation of results based on stress analysis. This capability allows for the removal or hiding of mesh elements that experience stress levels below a specified threshold, making it easier to focus on areas with higher stress concentrations. As demonstrated in Fig. 12, regions of low stress to none stressed presented in navy blue to sky blue colors are to be eliminated from model. The areas where the stress is mostly concentrated are presented in red moving to less stress which are presented in green which must be kept in the final model. We excluded or concealed the mesh areas with low stress and maintained the mesh regions that experience high stress or exceed a specified stress level resulting into the model in the Fig. 13. The optimized mesh file shown in Fig. 13 was then exported into another mesh file, and subsequently imported onto a separate, non-optimized orthosis model as Fig. 14a shows. To visualize non-stressed areas, we changed the transparency of the orthosis model to see the mesh imported from the previous results. This step gave us the opportunity to see the areas in which we do not have any mesh, which present the zones in which we can remove the material. We then removed the material using an elliptical shape to avoid stress concentrations, as shown in Fig. 14b, which presents the mesh over the optimized model. The optimized model is then depicted in Fig. 14c.

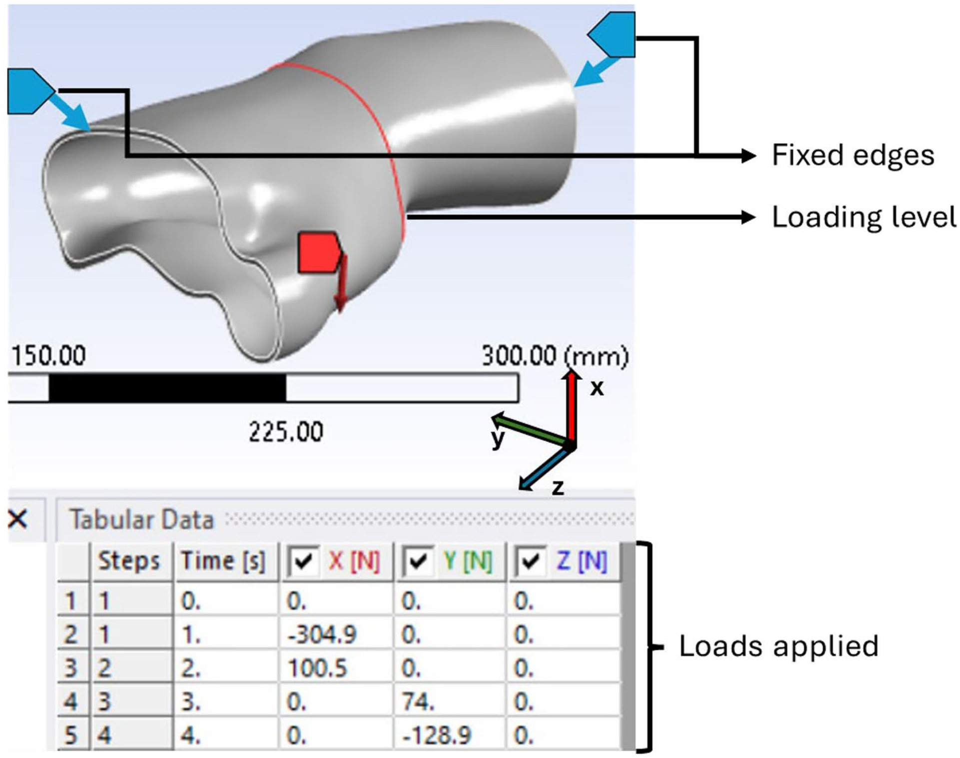

Fig. 11 Loads and boundary conditions applied on the orthosis

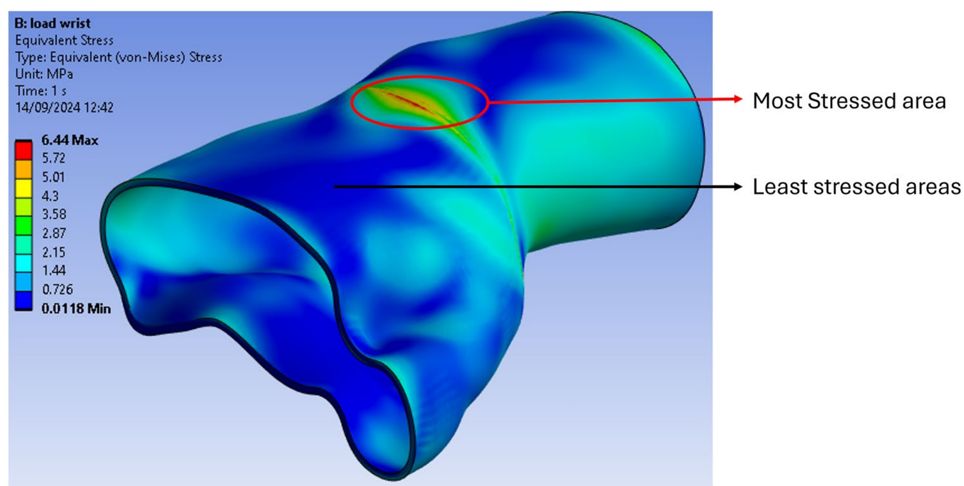

Fig. 12 Stress results of the orthosis simulation

2.6 RO manufacturing

To optimize the time and cost of the printed product, the printing parameters and the printing orientation must be carefully chosen. This may include adjusting the layer thickness, printing speed, and temperature, as well as considering the direction of the object in the build space to minimize the use of support material and reduce the overall printing time. This can also include the object's positioning in the build space to reduce the amount of support material required and increase the efficiency of the printing process. In our case, the optimal position for printing the orthosis is shown in Fig. 15. This allowed us to print it without any support material even for the removed materials areas. By reducing the printing speed of the outer shell, we don't have to add any support to these areas. And then, no cleaning, support removal and post processing to our orthosis after the manufacturing is needed. Which will gain us time to have the orthosis ready to use with a smooth surface quality. However, in this printing orientation, the material behaviour is the lowest (90°) for the flexion at the wrist level. We used the same white PLA material as used for printing the tensile test specimens, with a 100% infill density. We have chosen 0.15 mm layer height, 60 mm/min intern printing speed,

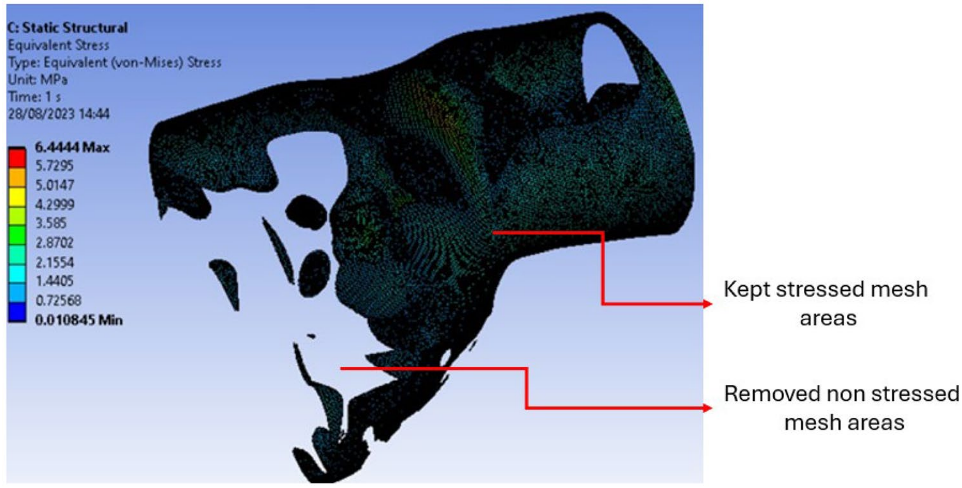

Fig. 13 None stressed areas elimination with the numerical results

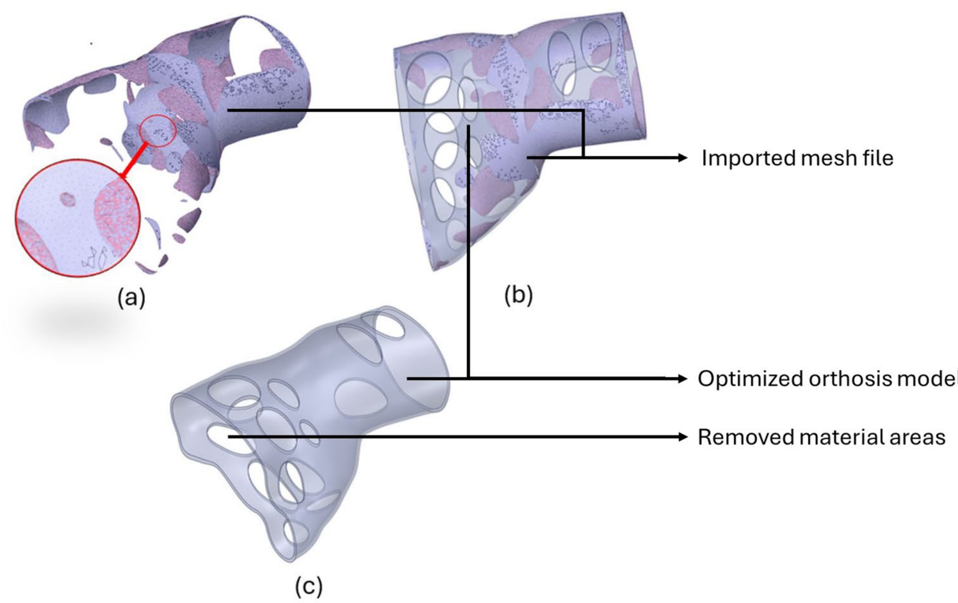

Fig. 14 The hand orthosis optimisation process (**a** imported mesh, **b** material removal from the orthosis model, **c** optimized hand orthosis)

and 30 mm/min for the outer and inner shells for high surface quality and optimal printing time. The supports for the orthosis were fabricated using a 3D printer and underwent a three-point bending test on the MTS 810 machine. The supports were securely fixated on the device to ensure stability during the experiment and prevent sliding of the orthosis.

2.7 RO strength-resistant experimental tests

ISO 22523:2006 [41] stands as the globally adopted standard for External Limb Prostheses and External Orthoses (ELPOs). It outlines criteria and testing procedures covering various aspects of ELPOs, encompassing durability, materials, usage limitations, risk assessment, and usage instructions. Notably, this standard does not include specific test conditions for wrist-hand orthoses. Consequently, we have opted for the three-point bending test to assess the durability of our wrist-hand orthosis. This test is standardized, dependable, precise, and relatively straightforward to execute.

The three-point bending test was conducted on an MTS 810 machine, with two tests performed. The flexion load was placed at the wrist level. The loading speed was 5 mm/min, moving downward vertically at the wrist level. The printed RO support for the test eliminated the movement freedom of the orthosis due to its shape. These supports were manufactured to be placed at a 50 mm distance from the flexion load. The first test revealed a defect in the orthosis's horizontal alignment, with an aligned angle of 11°, as shown in Fig. 16. This misalignment led to a slight sliding and a stress concentration at the left support level, ultimately causing the orthosis to fail. In comparison, the second test addressed this issue by correcting the alignment problem, reducing the

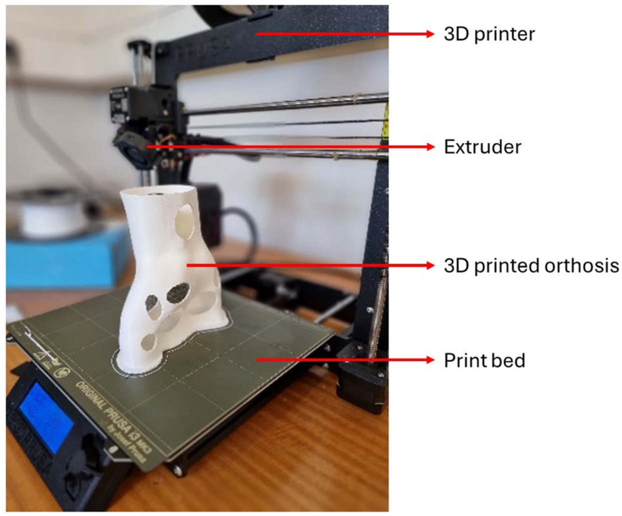

Fig. 15 The printed orthosis position in vertical building orientation

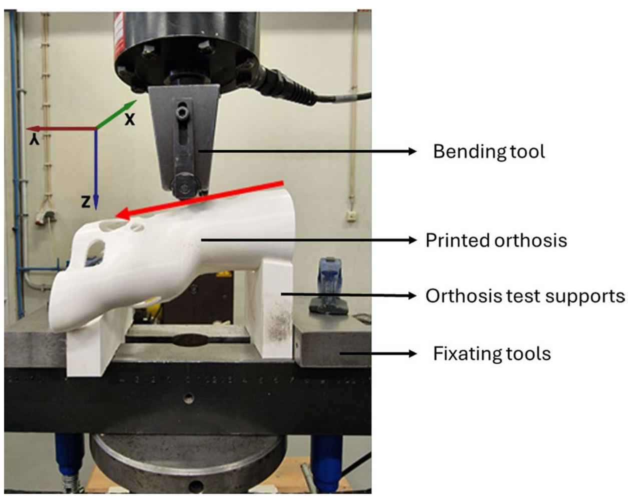

Fig. 16 First experimental 3-point bending test

angle to 2°, by modifying the support design and incorporating round edges to reduce the force concentration at specific areas. This improved alignment is depicted in Fig. 17. The study conducted three-point bending tests until the failure of the orthoses, and the outcomes of the experiments are presented through load–displacement curves.

3 Results

In this section, we will work on the different experimental results found in the investigations carried out, starting with the tensile tests made to extract the mechanical behaviour of the white PLA material that we used, going through the

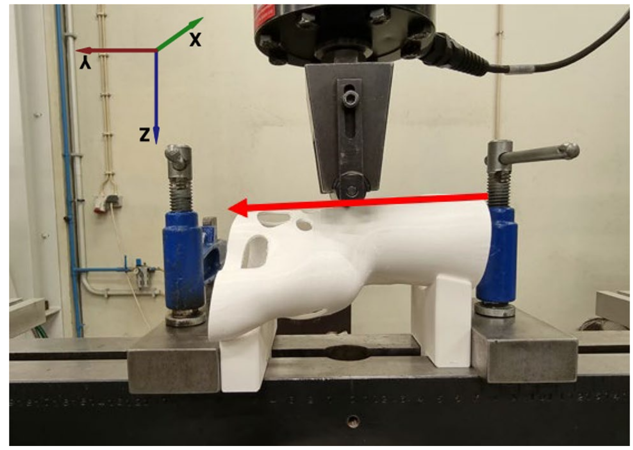

Fig. 17 Second experimental 3-point bending test

results found by the three-point bending tests made on the orthoses models, and finally presenting the results of the fitting and comfort tests.

3.1 Tensile tests results

The results are depicted in Fig. 18. The comparison of the elastic behaviour of various printing orientations revealed that while each exposure exhibited similar elastic behaviour, the 90° specimen displayed lower stress resistance. Notably, the strain at fracture differed significantly between the orientations, with the 90° specimen failing at a value of 0.02 and showing minimal plastic deformation. In contrast, both the 00° and 45°/– 45° specimens exhibited elastoplastic behaviour, with the 00° specimen failing at a value of 0.03 and the 45°/– 45° specimen failing at a value of 0.05. These results show that the best printing orientation is the 45°/– 45° which gives the best combination of stress and strain values while the 90° is the weakest orientation that has the lowest deformation and stress resistance and doesn't have any plastic deformation. This issue is caused by weak interlayer adhesion and structural instability resulting from the layers being deposited horizontally, which are perpendicular to the applied load during our tensile tests. In our numerical simulation, we used the 90° printing orientation for the material's mechanical behavior because the orthosis was printed vertically. This approach was chosen to reduce printing time and costs, as using the 45°/– 45° orientation would have required additional support material, increasing both the time and expense of the printing process. Additionally, since the orthosis is printed vertically, the load applied during testing is perpendicular to the printing orientation, aligning with the 90° tensile specimens.

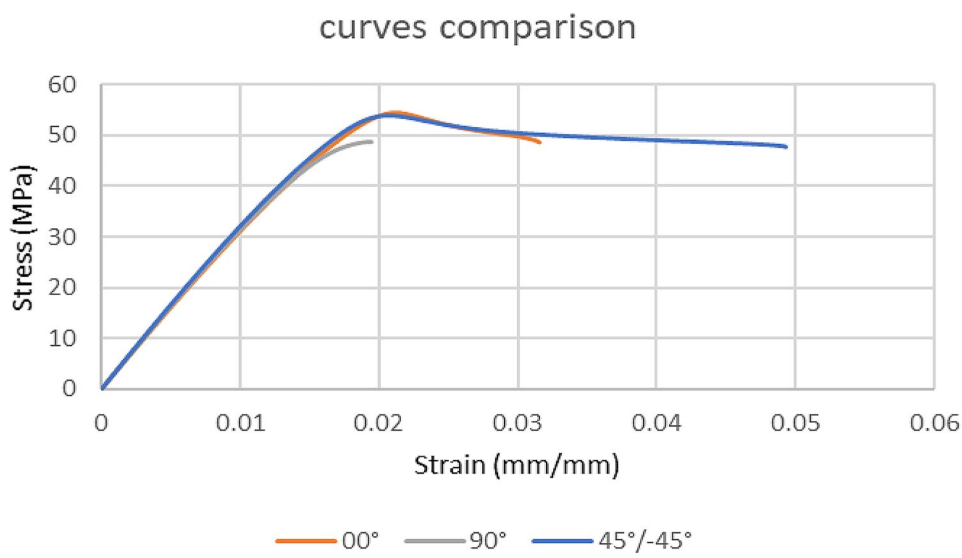

Fig. 18 Stress–strain curves for different printing orientations

3.2 RO experimental tests

The first orthosis test identified two major failure points, as depicted in Fig. 19. The first failure point, surrounded in red, was caused by a stress concentration at a weak spot and an acute part of the orthosis support, failing a force of 600 N. The second failure point, surrounded in green, was caused by a stress concentration at the support part and failed at a force of 1000 N. This test did not work as expected. The first failure point occurred at the support area due to the misalignment of the orthosis during the test, which caused the load force to concentrate mainly on the left side of the support. Additionally, the sharp edges of the supports used in the initial test contributed to the failure. We did not visualize any sign of failure at the wrist loading area which led us to the second test. In this test, we modified the supports by incorporating round edges to address this issue.

The orthosis alignment made with the support modifications improved performance regarding resistance to bending strength. The failure occurred in the expected bending area rather than a weak spot, as observed in the first test. The test curve shown in Fig. 20 illustrates three distinct failure points. The first point, which occurred at a force of approximately 600 N, was caused by a concentration of reaction force in a weak spot and is indicated by the red colouration in Figs. 18 and 19. The second failure point on the orthosis's lower side occurred for the same reason but at a higher force of 800 N, as indicated by the green colouration in the exact figures. The final failure point, at a force of approximately 1170 N, occurred in the overall orthosis and is indicated by the black colouration in the figures.

Additional details of the experimental test results can be found in the curve presented in Fig. 21.

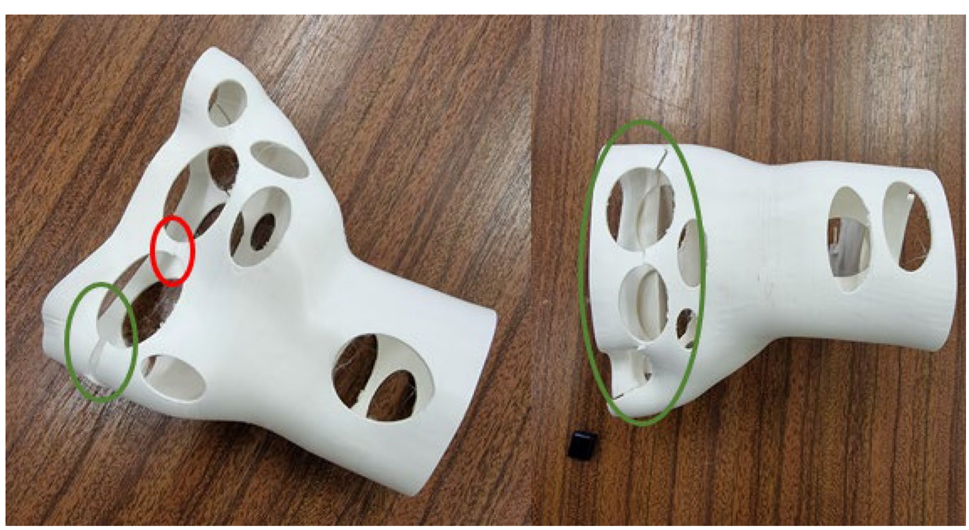

Fig. 19 Failure areas of the first test (red: first failure area, green: second failure area)

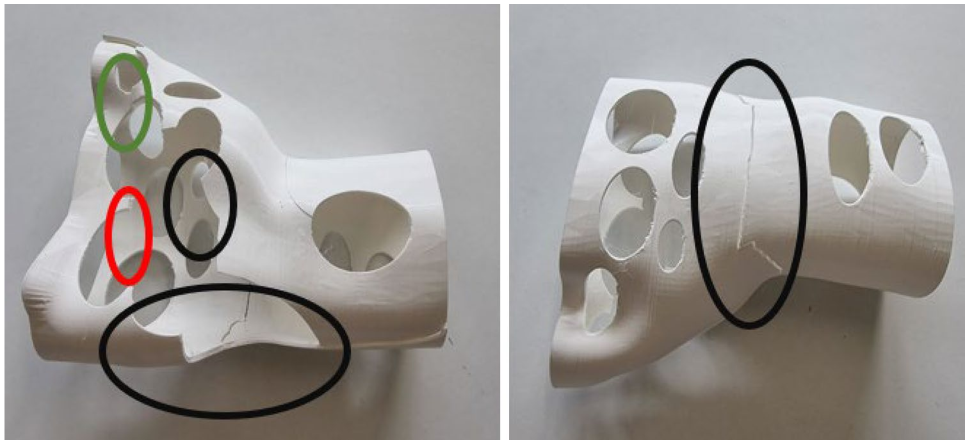

Fig. 20 Failure areas of the second test (red: first failure area, green: second failure area, black: third failure areas)

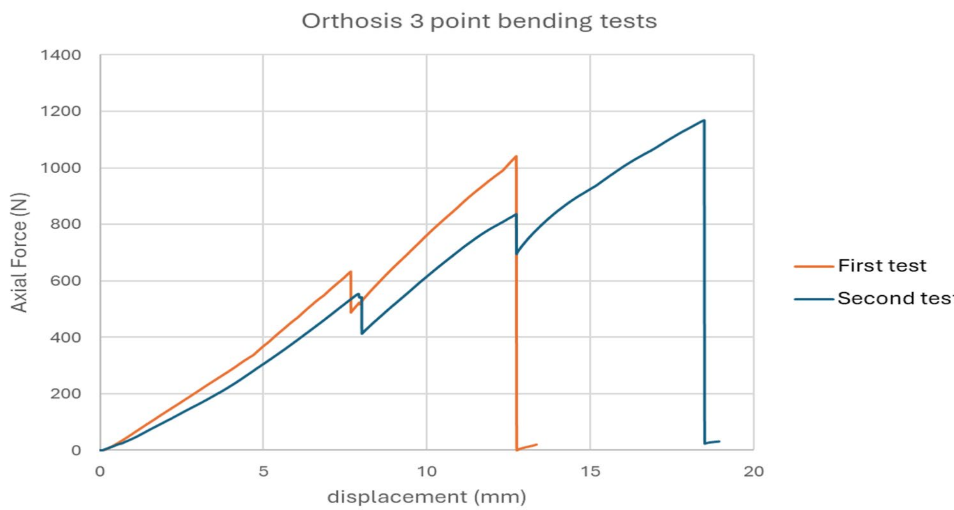

Fig. 21 Three-point RO bending tests—different axial forces in function of the displacements

The initial experimental test did not fail at the wrist level where the bending tool was applied, despite the results indicating that the orthosis could withstand up to 1030 N. This outcome prompted a second test to be conducted with improved alignment. The second test yielded similar failure points as the first, but the orthosis resisted the load until failure occurred at the wrist level where the bending tool was applied during the bending test. At this point, the orthosis exhibited a complete break, as depicted by the black circles in Fig. 20. The maximum load that the orthosis could sustain was 1170 N. This load resistance exceeds the typical requirements for orthosis applications. During our introduction, we found that wrist-hand orthoses do not need to bear loads higher than 300 N, as mentioned by F. Górski et al. [28]. Additionally, K. R. Holzbaur et al. [40] investigated that the maximal force generated during wrist movements is approximately 304.9 N.

Our topology optimization strategy enabled the fabrication of a high-resistance orthosis, demonstrating the acceptability of this design. The orthosis can withstand the loads exerted by the human body to maintain wrist stability and can even be employed for external load protection. However, the deformation that occurs at the load area must be considered. In our case, the orthosis experienced a deformation of 18 mm, which includes the cumulative deformations from various failure points at the maximum load applied (1170 N). These defects refer to the incremental deformations occurring as each failure point was reached. This deformation is not the deformation the orthosis was subjected to at the wrist level. It includes the deformations caused by failure points during the test. The true deformation at the wrist level is unknown and we need other tests to evaluate this point. However, maintaining a high load at the wrist level is the focus of this paper. By visualizing the curves, each failure occurred at nearly 6 mm from the previous one. This can be the deformation before failure of the orthosis at the wrist level too. The deformation is a significant factor to consider in the context of the orthosis's intended use. This could impact the functionality, fit and effectiveness of the orthosis during the recovery process. Therefore, it is essential for clinicians to specify the maximum allowable deformation under a given load. The orthosis thickness is a parameter that we can manipulate to have higher resistance and lower deformation to have the demanded rigidity of the orthosis.

3.3 Fitting and comfort tests

We investigated various possibilities to design an orthosis that is easy to assemble and disassemble as needed by the user. Through this investigation, we determined that the most effective solution would be to divide the orthosis into two parts and implement a Snap-Fit design on each side. The design was optimized for resistance, durability, and ease of use. Additionally, we conducted comfort and fitting tests to ensure that the design was functional and practical for the intended use by putting the orthosis on moving the wrist for possible movement and trying its fitting, assembly, and disassembly. The results of these efforts are presented in Fig. 22. Furthermore, the design was improved to be visually pleasing, and patients also had the option to select their preferred printing colour for added satisfaction. The patient can also easily open and close it by himself. Overall, our design aims to enhance the usability and satisfaction of orthotic devices for patients.

4 Discussion

The main objective of this work is to manufacture a customized RO that provides high performance while keeping the hand comfortable and breathable. Our study also addressed the orthosis quality, cost, and manufacturing time. The quality was improved by providing more airing area on the orthosis, following the stress it will be subjected to. Cost and time were evaluated by optimizing the topology, which reduced the material and time required for manufacturing. Additionally, we chose the right parameters, such as the building position, which did not require any support materials, thus reducing the printing time. The second goal was to choose the best method for the entire process, which included reverse engineering, CAD modeling, and FDM technology, known for being cost-effective and time-efficient. We also utilized tensile tests to extract the material properties in different printing orientations and incorporated these properties into our simulation process. This allowed us to optimize the orthosis topology based on the loads it would be subjected to.

For the scanning process, our model does not require a high-accuracy scan but a good post-scanning process to have a smooth model. Also, the posture of the scan has a significant impact on the model. We had to find a position where we could continuously scan our hands without obstacles for more details acquisition. The 3D model we saw with the scanning process was acceptable and took 15 min.

After the scan, a CAD modelling strategy was used, which can be automated in the future. These steps took around half an hour on an average laptop, resulting in the first RO model in which we can manipulate the thickness depending on our need for stress resistance. In our case, we started with a 2-mm thickness. Once we create the first model, the FEM will be next. Thus, it is necessary to have the mechanical properties of our material. However, the 3D printing materials properties need to be provided correctly, and an anisotropic behaviour will be present in our printed part, leading us to investigate the PLA material used.

The previous tensile test results show that our case's favourable printing orientation is the 45°/– 45° printing orientation. However, due to the thin wall of our orthosis, the

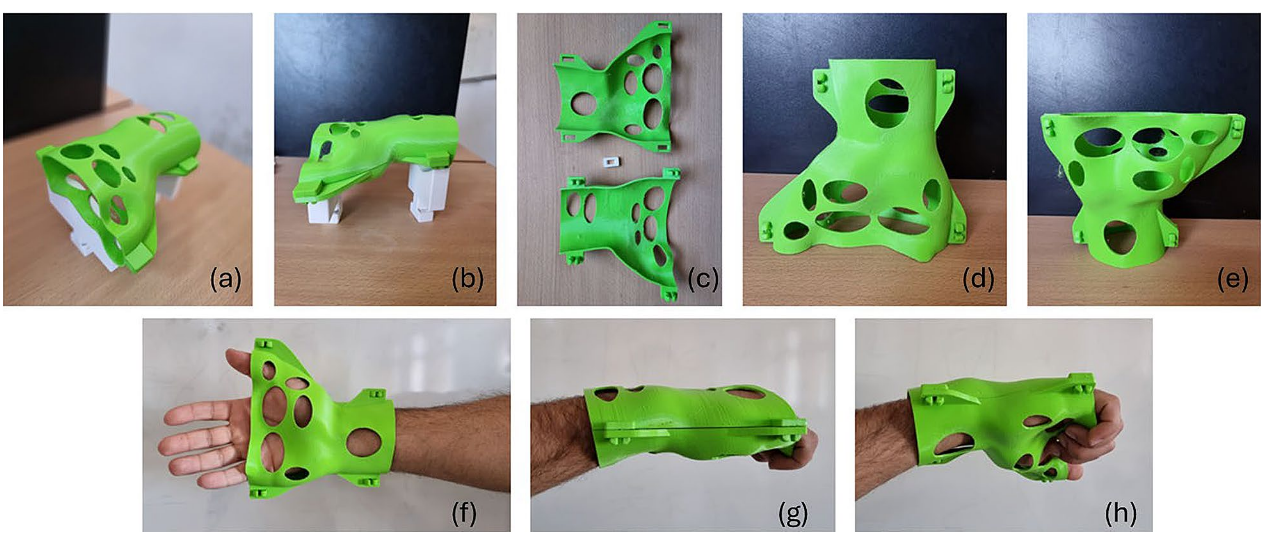

Fig. 22 The optimized orthosis final result. **a–e** Detailed views of various parts of the orthosis, highlighting its design features and functionality; **f–h** fitting tests of the orthosis, demonstrating its application and fit

printing strategy would not impact the strength of our orthosis but the orthosis position. The printing position should be horizontal for more stress resistance, but this position will cause a high material consumption for the support required, thus more printing time and higher cost. For the vertical position that does not require any support material, the printing of the complete orthosis will pass from 70 to 18 h, but the stress resistance on the wrist level will be the weakest. We have chosen the vertical printing position and investigated the orthosis printed on that position. That led us to use the 90° specimens behaviour in the FEM for the topology optimisation.

The topology optimization was a significant gain using ANSYS Workbench due to its rapid and easy manipulation. By importing our model, the mechanical behaviour of our PLA material extracted from the tensile test, and applying the necessary boundary conditions, the numerical simulation took around 10 min using a quadratic 1 mm mesh size. The results are those of a flexion force load applied at the wrist level, an approach to the experimental test made during our work. The optimisation that has been made was done following the results found by the load.

The orthosis manufacturing process can be designed to provide different levels of support and resistance based on the wearer's needs. Depending on the objective, such as alignment, movement support, resistance, weight support, or protection, the appropriate manufacturing process, materials, and geometry will be chosen [7]. The requirements for the orthosis will be established based on the specific application for which it will be used. In our case, we worked on a rigid orthosis that needs to resist to the joint movement [42]. Thus, it needs to be able to fixate the wrist movement by resisting to a certain load and needs to be comfortable and custom fit to the user.

The experimental tests on the orthosis showed that if tested properly, the orthosis can maintain up to 1170 N with only 2 mm thickness, which is more than required by a RO, as stated by F. Górski et al. [28], with the help of experts such as physiotherapists and orthopedists, that in practice, the RO does not have to bear a load higher than 300 N. By comparing our findings with the results of F. Górski et al. [28], we found out that their results are close to our results. For the strength testing, their best orthosis resisted against a load of 1328 N for the vertical printing position using PLA material, while our orthosis resisted against 1170 N for the vertical printing direction. Also, we are using a lower layer thickness for higher accuracy and better surface quality (0.15 mm compared to 0.3 mm of Górski’s orthosis). We could have an orthosis with a similar resistance but with lower thickness due to the topology optimisation done following numerical simulation results of an approximate load that can be applied to the orthosis during its operation.

This, despite all the different experimental conditions between our two flexion tests, which are:

- Different orthosis thickness: their orthosis has a 4 mm thickness, while ours has a 2 mm thickness.
- A forearm phantom (Fig. 1) supports their orthosis, which improves the orthosis resistance.

During the test, our orthosis had no internal support; this proves the effectiveness of our topology optimisation strategy using the numerical simulation.

The present research investigated a unified, topology-optimized orthosis design with the aim of minimizing its weight. The final design included a snap-fit mechanism to facilitate assembly and disassembly during testing of the orthosis fit. Despite this method has usability benefits, its implementation requires more research to understand its effect on overall stiffness. To guarantee the required stiffness of the final design, further research will use mechanical tests or simulations to assess the mechanical reaction of the snap-fit design. This analysis is essential for refining the design to achieve the necessary rigidity. By examining different snap-fit configurations, our goal is to develop a mechanism that provides exceptional stiffness and ensures it does not fail before the orthosis itself during flexion testing or during use.

5 Conclusion

In conclusion, this study successfully achieved the primary objectives of designing and 3D printing a customized wrist-hand orthosis (RO) that prioritizes high performance, optimal fit, and practical usability while considering cost and manufacturing time. User comfort was evaluated through detailed fitting tests on the patient, ensuring that the orthosis provided the necessary support without causing discomfort. Additionally, design features such as increased airflow and an optimized topology were incorporated to enhance overall comfort and practicality for the user. The utilization of 3D scanning combined with 3D printing technology, complemented by finite element analysis (FEM) for topology optimisation, proved to be a practical approach. Notably, investigating the PLA material properties and printing orientations contributed to optimising the orthosis's mechanical performance. The experimental tests demonstrated exceptional load-bearing capabilities, surpassing relevant RO requirements. Moreover, a comparison with prior research highlighted the efficiency of this study's design. Looking ahead, the insights gained from this work can be extended to explore orthotic and prosthetic applications for different body parts, leveraging similar strategies and numerical simulations to validate further and enhance the outcomes of this research, thereby advancing the field of customized medical devices.

The key findings of our research are presented in the following bullet points:

- **Utilization of Technology:** The utilization of 3D scanning combined with 3D printing technology, complemented by finite element analysis (FEM) for topology optimization, proved to be a practical approach for the modeling of a customized RO orthosis.
- **Material Properties:** Investigation of the PLA material properties with different printing orientations contributed to optimizing the orthosis's mechanical properties in our simulations.
- **Load-Bearing Capabilities:** The experimental tests demonstrated exceptional load-bearing capabilities, surpassing relevant RO requirements.
- **Comparison with Literature:** Compared to other findings in the literature, our orthosis performed nearly the same load bearing with a 2 mm thickness compared to other orthoses with a 4 mm thickness.
- **Snap-Fit Mechanism:** The integration of the snap-fit mechanism in our orthosis allowed for easy assembly and disassembly.
- **User Comfort and Design Features:** The orthosis performed well in fitting tests on the patient, ensuring that the orthosis provided the necessary support without causing discomfort. Design features such as increased airflow and an optimized topology were incorporated to enhance overall comfort and practicality for the user.

In future, we will work on different body orthoses, such as the ankle–foot orthosis, knee orthosis, or neck orthosis, using the same methodology and technology. We will also explore the possibility of extending this work to prosthesis manufacturing, such as artificial limbs or joints, which may require more complex design and fabrication processes. Also, it is planned to investigate different materials or composites that have better mechanical properties, biocompatibility, and durability than PLA.

Declarations

Conflicts of interest The authors declare no conflict of interest.

References

1. Berry DA (1987) Composite materials for orthotics and prosthetics. J Prosthetists Orthot 40(4):35–43
2. Kuettel D (2016) Pulley optimization for a walking-engine-actuated active ankle-foot orthosis. J Young Investig 31(5):32–38. https://doi.org/10.22186/jyi.31.5.32-38
3. Miro RM, Lewandowski AL, Kahle JT, Mengelkoch LJ, Boone DA, Highsmith MJ (2013) Bibliometric analysis of articles published from 2009 through 2011 in the journal of prosthetics and orthotics, journal of the American academy of orthotists and prosthetists. J Prosthetics Orthot 25(4):201–208. https://doi.org/10.1097/JPO.0000000000000007
4. Savov I, Todorov G, Sofronov Y, Kamberov K (2019) Research and development of methods and tools for rapid digital simulation and design of personalized orthoses. In: Zahariev E, Cuadrado J (eds) IUTAM Symposium on Intelligent Multibody Systems – Dynamics, Control, Simulation. IUTAM Bookseries, vol 33. Springer, Cham. https://doi.org/10.1007/978-3-030-00527-6_8
5. Wu D, Lane Thames J, Rosen DW, Schaefer D (2013) Enhancing the product realization process with cloud-based design and manufacturing systems. J Comput Inf Sci Eng. https://doi.org/10.1115/1.4025257
6. Gailey R, Allen K, Castles J, Kucharik J, Roeder M (2008) Review of secondary physical conditions associated with lower-limb amputation and long-term prosthesis use. J Rehabil Res Dev 45(1):15–30. https://doi.org/10.1682/JRRD.2006.11.0147
7. Santos S, Soares B, Leite M, Jacinto J (2017) Design and development of a customised knee positioning orthosis using low cost 3D printers. Virtual Phys Prototyp 12(4):322–332. https://doi.org/10.1080/17452759.2017.1350552
8. Kumar V, Bajcsy R, Harwin W, Harker P (1996) Rapid design and prototyping of customized rehabilitation aids. Commun ACM 39(2):55–61. https://doi.org/10.1145/230798.230804
9. Wang Y, Tan Q, Pu F, Boone D, Zhang M (2020) A review of the application of additive manufacturing in prosthetic and orthotic clinics from a biomechanical perspective. Engineering 6(11):1258–1266. https://doi.org/10.1016/j.eng.2020.07.019
10. Chen RK, Jin Ya, Wensman J, Shih A (2016) Additive manufacturing of custom orthoses and prostheses—a review. Addit Manuf 12:77–89. https://doi.org/10.1016/j.addma.2016.04.002
11. Herr H (2009) Exoskeletons and orthoses: Classification, design challenges and future directions. J Neuroeng Rehabil 6(1):1–9. https://doi.org/10.1186/1743-0003-6-21
12. Chen CL, Tai BL, Wang Y, Shih AJ, Wensman J (2014) Additive manufacturing of personalized ankle-foot orthosis. Trans N Am Manuf Res Inst SME 42(January):381–389
13. Banga RHK, Belokar RM, Kalra P, Kumar (2018) Fabrication and stress analysis of ankle foot orthosis with additive manufacturing. Rapid Prototyp. J. 24(2):301–312. https://doi.org/10.1108/RPJ-08-2016-0125
14. Pallari JHP, Dalgarno KW, Woodburn J (2010) Mass customization of foot orthoses for rheumatoid arthritis using selective laser sintering. IEEE Trans Biomed Eng 57(7):1750–1756. https://doi.org/10.1109/TBME.2010.2044178
15. Faustini MC, Neptune RR, Crawford RH, Stanhope SJ (2008) Manufacture of passive dynamic ankle-foot orthoses using selective laser sintering. IEEE Trans Biomed Eng 55(2):784–790. https://doi.org/10.1109/TBME.2007.912638
16. South BJ, Fey NP, Bosker G, Neptune RR (2010) Manufacture of energy storage and return prosthetic feet using selective laser sintering. J Biomech Eng 132(1):1–6. https://doi.org/10.1115/1.4000166
17. Schrank ES, Hitch L, Wallace K, Moore R, Stanhope SJ (2013) Assessment of a virtual functional prototyping process for the rapid manufacture of passive-dynamic ankle-foot orthoses. J Biomech Eng 135(10):1–7. https://doi.org/10.1115/1.4024825
18. Gibson I, Rosen DW, Stucker B (2010) Additive manufacturing technologies: Rapid prototyping to direct digital manufacturing. Springer New York, NY. https://doi.org/10.1007/978-1-4419-1120-9

19. Cha YH et al (2017) Ankle-foot orthosis made by 3D printing technique and automated design software. Appl Bionics Biomech. https://doi.org/10.1155/2017/9610468
20. Berke GM et al (2010) Comparison of satisfaction with current prosthetic care in veterans and servicemembers from vietnam and OIF/OEF conflicts with major traumatic limb loss. J Rehabil Res Dev 47(4):361–372. https://doi.org/10.1682/JRRD.2009.12.0193
21. Han P (2017) Additive design and manufacturing of jet engine parts. Engineering 3(5):648–652. https://doi.org/10.1016/J.ENG.2017.05.017
22. Ali MH, Smagulov Z, Otepbergenov T (2021) Finite element analysis of the CFRP-based 3D printed ankle-foot orthosis. Proc Comput Sci 179(2020):55–62. https://doi.org/10.1016/j.procs.2020.12.008
23. Sood AK, Ohdar RK, Mahapatra SS (2010) Parametric appraisal of mechanical property of fused deposition modelling processed parts. Mater Des 31(1):287–295. https://doi.org/10.1016/j.matdes.2009.06.016
24. Górski F, Kuczko W, Wichniarek R, Hamrol A (2018) Mechanical properties of composite parts manufactured in FDM technology. Rapid Prototyp J 24(8):1281–1287. https://doi.org/10.1108/RPJ-11-2016-0197
25. Casavola C, Cazzato A, Moramarco V, Pappalettere C (2016) Orthotropic mechanical properties of fused deposition modelling parts described by classical laminate theory. Mater Des 90:453–458. https://doi.org/10.1016/j.matdes.2015.11.009
26. Vaes D, Van Puyvelde P (2021) Semi-crystalline feedstock for filament-based 3D printing of polymers. Progress Polym Sci. https://doi.org/10.1016/j.progpolymsci.2021.101411
27. Beckennan H, Becher J, Lunkhorst GJ, Verbeek ALM (1996) Walking ability of stroke patients: efficacy of tibia1 nerve blocking and a polypropylene ankle-foot orthosis, vol 77, no 11, pp 1144–1151. https://doi.org/10.1016/S0003-9993(96)90138-0
28. Górski F, Wichniarek R, Kuczko W, Zukowska M, Lulkiewicz M, Zawadzki P (2020) Experimental studies on 3D printing of automatically designed customized wrist-hand orthoses. Materials (Basel). https://doi.org/10.3390/ma13184091
29. Rybarczyk J, Kuczko W, Wichniarek R, Górski F, Żukowska M (2022) Study of individualized leg orthoses made by 3D printing of composite material, pp 10–11
30. Kumar R, Kumar M, Chohan JS (2021) The role of additive manufacturing for biomedical applications: a critical review. J Manuf Process 64(February):828–850. https://doi.org/10.1016/j.jmapro.2021.02.022
31. Graupner N, Herrmann AS, Müssig J (2009) Natural and man-made cellulose fibre-reinforced poly(lactic acid) (PLA) composites: an overview about mechanical characteristics and application areas. Compos Part A Appl Sci Manuf 40(6–7):810–821. https://doi.org/10.1016/j.compositesa.2009.04.003
32. Dal Maso A, Cosmi F (2019) 3D-printed ankle-foot orthosis: a design method. Mater Today Proc 12:252–261. https://doi.org/10.1016/j.matpr.2019.03.122
33. Sabyrov N, Sotsial Z, Abilgaziyev A, Adair D, Ali MH (2021) Design of a flexible neck orthosis on Fused Deposition Modeling printer for rehabilitation on regular usage. Proc Comput Sci 179:63–71. https://doi.org/10.1016/j.procs.2020.12.009
34. Leite M, Soares B, Lopes V, Santos S, Silva MT (2019) Design for personalized medicine in orthotics and prosthetics. Procedia CIRP 84:457–461. https://doi.org/10.1016/j.procir.2019.04.254
35. Durfee WK, Iaizzo PA (2018) Medical applications of 3D printing. Elsevier Inc. https://doi.org/10.1016/B978-0-12-813068-1.00021-X
36. Davide Felice Redaelli GC, Storm FA, Biffi E, Reni G (2019) Virtual design process to produce scoliosis braces by additive manufacturing. In: International Conference on design tools and methods in industrial engineering, 2019, pp 860–870.
37. Buonamici F et al (2018) A CAD-based procedure for designing 3D printable arm-wrist-hand cast. Comput Aided Des Appl 16(1):25–34. https://doi.org/10.14733/cadaps.2019.25-34
38. Baronio G, Harran S, Signoroni A (2016) A critical analysis of a hand orthosis reverse engineering and 3D printing process. Appl Bionics Biomech. https://doi.org/10.1155/2016/8347478
39. Vidakis N, Vairis A, Petousis M, Savvakis K, Kechagias J (2016) Fused deposition modelling parts tensile strength characterisation. Acad J Manuf Eng 14(2):87–94
40. Holzbaur KRS, Murray WM, Delp SL (2005) A model of the upper extremity for simulating musculoskeletal surgery and analyzing neuromuscular control. Ann Biomed Eng 33(6):829–840. https://doi.org/10.1007/s10439-005-3320-7
41. ISO 22523:2006 External limb prostheses and external orthoses. Requirements and test methods. British Standards Institution, 1st ed. [Online]. Available: https://www.iso.org/standard/37546.html. Accessed 26 Jul 2022
42. Aranceta-Garza A, Ross K (2021) A comparative study of efficacy and functionality of ten commercially available wrist-hand orthoses in healthy females: wrist range of motion and grip strength analysis. Front Rehabil Sci. https://doi.org/10.3389/fresc.2021.687554
43. Hosford W, Caddell R (2007) Metal forming: mechanics and metallurgy. Cambridge University Press (**ISBN 0-5218-8121-8**)